Polymer 51 (2010) 2918–2926

Contents lists available at ScienceDirect

Polymer

journal homepage: www.elsevier.com/locate/polymer

# Effect of particle diameter on the permeability of polypropylene/$SiO_2$ nanocomposites

V.N. Dougnac*, R. Alamillo, B.C. Peoples, R. Quijada*

*Departamento de Ingeniería Química y Biotecnología, Facultad de Ciencias Físicas y Matemáticas and Centro para la Investigación Avanzada de Materiales (CIMAT), Universidad de Chile, Casilla 2777, Santiago, Chile*

ARTICLE INFO

*Article history:*
Received 20 December 2009
Received in revised form
29 January 2010
Accepted 7 February 2010
Available online 12 February 2010

*Keywords:*
Polypropylene nanocomposites
Permeability
Silica nanospheres

ABSTRACT

In this contribution the permeation behaviour of polypropylene composites containing silica nanospheres of different diameters is reported. The composite materials were produced by melt compounding polypropylene with silica nanospheres, with diameters ranging from 12 to 150 nm, produced using standard sol–gel methods. The permeability of $O_2$, $N_2$ and $H_2O$ through the materials was tested. The results indicate that the addition of nanospheres with diameters of $\geq$30 nm results in an increase in the $O_2$ and $N_2$ permeability and is directly proportional to the nanosphere diameter. In the case of the water vapour transmission rate, it was found that there is also an increase, but the effect is inversely related with the nanospheres diameter. Incorporation of spheres with a diameter of 12 nm produces a decrease in the permeability of polypropylene composites in all instances, due to its formation of aggregates in composites.



## 1. Introduction

Polyolefin materials have grown to occupy an increasingly large role in our society, and are present in many aspects of our daily lives, the facile and inexpensive manufacture of these materials possessing a large range of physical properties has allowed them to displace older, less adaptable, and more expensive materials. Advances in nanoscience have allowed the range of properties in polyolefins to be tailored, particularly as a result of the generation of novel materials termed nanocomposites. These materials are formed through the addition of an inorganic phase, having at least one dimension measuring less than 100 nm, to a polymeric matrix. When effectively combined, these new materials possess distinct properties compared to the constituent parts [1,2]. Polyolefin composites, such as those formed from polyethylene and polypropylene, are of particular interest as they allow inexpensive, commodity polymers to be used across a wider range of applications than they would normally be suited [1]. Composite materials generated by mixing polymers with inorganic fillers in attempts to enhance the material properties have been under development for more than a century [3]. Such early attempts to modify polymer properties were successful in that the resulting materials possessed increased toughness and durability. The fillers used, however, had an inherent, natural form which was not necessarily optimised for the reinforcement of the composite.

Advances in polymer physics and synthesis have shown that the form and dimensions of the materials incorporated play a critical role in their efficacy in modifying the properties of the materials produced [4,5]. Originally, bulk materials such as clays, carbon black, calcium carbonate, and talc where used extensively in polymer composites [6,7]. It was realized, however, that similar results could be achieved using lower weight loadings if the inorganic portion was of smaller dimensions and well dispersed. Selecting natural materials with nanoscale dimensions such as clays, talc, silica, alumina, magnesium hydroxide and calcium carbonate [4,8–10] allows for the production of quality nanocomposites. These materials, however, are limited by the form and dimensions in which they occur naturally, limiting a key variable which can be modified to probe their effects in polymer matrices. Advances in synthetic inorganic materials chemistry have resulted in the development of numerous methods to construct inorganic materials with a diverse range of chemical compositions such as; $TiO_2$, $MoS_2$, $SiO_2$ among others in a variety of shapes and sizes, including sheets [11], spheres [12], fibres [13] and cubes [14]. The sol–gel method for generating silica structures is of particular interest as the resulting structures can be generated in a variety of forms and sizes [12,15–18]. The variation in shape and size can be accomplished via the modification of reaction conditions, such as the pH, water/metal alkoxide ratio, reaction temperature and time,

* Corresponding authors. Tel.: +56 2 9784188; fax: +56 2 6991084.
*E-mail addresses:* vdougnac@icaro.dic.uchile.cl (V.N. Dougnac), raquijad@ing.uchile.cl (R. Quijada).

0032-3861/$ – see front matter © 2010 Elsevier Ltd. All rights reserved.
doi:10.1016/j.polymer.2010.02.014

and also through the addition of surfactants and templating agents. A particular advantage of silicate materials is that they can be prepared inexpensively and with high purity. In addition, the materials do not have significant side reactions with polyolefin matrices, which allows for the evaluation of the effect of filler size and form directly without concerns about secondary interactions with the filler. As polypropylene is one of the principle materials used in the packaging industry [19,20], the modification of its permeation properties is of great interest. Numerous studies related to the modification of polypropylene barrier properties have been reported in the literature, however while clays and other layered materials have been extensively studied [19,21–26], the effect of nanosphere incorporation on the permeability of composite materials has not received much attention. Much of the literature discusses the use of glassy polymers, which are useful for gas separation membranes, and address the use of nanospheres (or nanosilicas of indeterminate shape) [27,28]. These composites have high weight loadings, typically 10–30 wt% silica. In these materials, the permeation behaviour of the composites depends greatly on the chemical compatibility of the silica particles with the polymer matrix. When the silica particles were chemically modified to be compatible with the polymer matrix it was found that their presence reduced the permeability of the composites. However, when the silica particles where incorporated without surface treatment the permeability increased, due to the formation of voids around the nanoparticles through which gases could freely permeate [29,30]. It has been shown that silica nanoparticle weight loading has a large effect on the permeability of iPP composites; composites with 1 wt% loading producing a small reduction in permeability compared to the polymer matrix, while those with 10 wt% silica had a ca. 30% decrease in permeability. In addition, the authors noted that the selectivity of the materials changed as a function of weight loading with the permeability of oxygen decreasing less than that of nitrogen [31]. The effect of nanosphere diameter on the permeability of polypropylene nanocomposites has been studied even less, and often only via theoretical methods [32–34].

While polypropylene is one of the most commonly used polymers in consumer applications, the permeability behaviour of its composites with silica nanospheres has not been extensively studied and the effect of diameter even less so. It was suspected that due to their low cost, high purity and the expected ability to alter the permeation of these materials that they would have potentially use in the packaging industry. Therefore, in this work the effect of adding silica nanospheres of varying diameters, to a polypropylene matrix on the permeability of oxygen, nitrogen and water vapour was studied. In addition, the physical and thermal properties of the resulting composites were evaluated.

## 2. Experimental

### 2.1. Materials

Polypropylene with melt flow indexes (MFIs) of 26 g/10 min (PP26) and 13 g/10 min (PP13) and molecular weights of 150,000 and 250,000 g/mol respectively were obtained from Petroquim Chile and used as received. The antioxidant used in the preparation of the composite materials was a mixture (2:1) of Irgafox 1010 and Irganox 168. Polybond 3150, a maleic anhydride (MA) graft copolymer of polypropylene, PP-g-MA, with 1 wt% MA and an MFI of 56, was used as a compatibilizer. Tetraethylorthosilicate (≥98%, TEOS) and octadecylamine (90%, ODA) were purchased from Sigma–Aldrich and used as received. Ammonia (25%) was acquired from Merck, and ethanol (96%) from Equilab.

### 2.2. Synthesis of silica nanospheres via sol–gel method

The nanospheres were produced using a two solution method. The first solution contained a mixture of water, ammonia, octadecylamine and ethanol, while the second solution consisted of TEOS in ethanol. The composition of the first solution was varied in an attempt to control the size of the final nanoparticles, and the quantities of each reagent used are given in Table 1. The solutions were stirred at 40 °C for 30 min to ensure that the ODA was fully dissolved. The second solution was stirred at 40 °C and added drop wise into the rapidly stirring solution 1. The resulting solution was sealed and allowed to stir for 2 h. The solvent was then evaporated at 80 ± 10 °C. A fine white powder was obtained which was dried in a vacuum oven for 20 h at 130 ± 10 °C. Finally, the powder was homogenized using an analytical mill at 5.0 ± 0.1 °C.

### 2.3. Polymer blending

The polypropylene/$SiO_2$ nanocomposites were produced by direct melt mixing in a Brabender at 190 ± 2 °C, 110 rpm, for 8 min under a nitrogen atmosphere and then flattened in cold hydraulic press to produce a sheet ca. 5 mm thick before solidifying. Each mixture had a mass of approximately 35 g, composed of 30 g polypropylene, a small spoonful (ca. 30 mg) of Irganox 1010: Irgafox 168 (2:1) antioxidant; 4.22 g of Polybond 3150, and sufficient isolated product from 2.2 to achieve a loading of 1 wt% of filler. The materials were mechanically mixed and added directly to the running, preheated and purged Brabender. Mixtures of the polypropylenes with polybond were produced using the same proportions (without silica filler) and used as a control for comparison purposes.

### 2.4. Thermal analysis

Thermal analysis of the blended materials was conducted using a TA instruments Differential Scanning Calorimeter model 2920 at a heating rate of 10 °C/min. The data reported are from the second cycle to eliminate any thermal history. The crystallinity of the samples was calculated by using the $\Delta H_m$ for pure, crystalline iPP 165 J/g [35].

### 2.5. Mechanical property testing

The polymer samples were prepared for tensile testing by melt pressing the samples at 20 °C above the melting temperature of the material at 50 bar for 5 min in a heated hydraulic press. The specimens were cooled under pressure by flushing the press with cold water. Testing specimens were then cut from these sheets using a heated stainless steel die, with dimensions of 30 × 5 mm and thickness of 0.2 mm, and a hydraulic press. A minimum of 5 specimens were cut from each sheet, the 3 most homogeneous samples were selected for testing. The mechanical properties were

**Table 1**
Synthesis conditions and nanosphere sizes.

| Sample | Ethanol (mL) | ODA (mmol) | Total volume (mL) | Sphere diameter (nm) |
|---|---|---|---|---|
| 1 | 45 | 0.297 | 50.05 | 12 |
| 2 | 45 | 1.187 | 50.05 | 30 |
| 3 | 45 | 0.890 | 50.05 | 36 |
| 4 | 45 | 0.594 | 50.05 | 44 |
| 5[a] | 90 | 0.594 | 100.1 | 70 |
| 6 | 55 | 2.968 | 60.05 | 150 |

TEOS: 3 mL; Water: 2.05 mL.
[a] TEOS: 6 mL, Water: 4.1 mL.

measured using an HP D500 dynamometer at a rate of 50 mm/min at 23 ± 1 °C. The Young's modulus was found by calculating the slope of the stress–strain curve after the initial toeing region. The stress at break is defined as the last point prior to the precipitous drop in strain associated with the sample breaking.

### 2.6. Permeability

Samples for permeability testing were produced by melt pressing the samples at 190 °C to a thickness of approximately 0.20 mm. Circles (ca. 2 cm diameter) from the most homogeneous regions of the films were cut out to fit into the permeability cell.

The permeability of the polymeric materials was evaluated using a permeation cell built in our laboratory, whose design is described elsewhere [36,37]. The permeation equipment consisted of a low pressure and a high pressure side, whose pressures were constantly monitored using 300 mBar and 16 bar pressure sensors attached to a Dickson data logger. The high pressure side was equipped with a pressure reservoir which had a volume of 500 mL (roughly 25 times the volume of the low pressure side). The permeation cell and pressure reservoir were maintained at a constant temperature (30 °C). Samples were cleaned using acetone and then mounted into the cell. The cell was sealed and both sides of the equipment exposed to vacuum ($10^{-3}$ bar) overnight. The high pressure side of the cell was exposed to 1–2 bar of nitrogen or oxygen pressure and the permeation across the polymer measured by monitoring the pressure increase on the other side of the film. Once steady state conditions were achieved, the permeability was calculated using equation (1) [29].

$$P = \frac{273}{76}\left(\frac{V_b I}{A T p_a}\right)\frac{dp_b}{dt} \quad (1)$$

where $V_b$ is the volume of the low pressure side of the setup, $I$ is the thickness of the polymer film, $A$ is the effective area of the polymer film, $p_a$ is the pressure of the applied gas on the high pressure side, $dp_b/dt$ is the slope of the pressure/time curve after the system has reached a steady state (linear region), $T$ is the absolute temperature. $P$ is expressed in barrers, 1 barrer = ($10^{-10}$ $cm^3$(STP) cm/$cm^2$ s cm Hg).

### 2.7. Water vapor transmission

The water vapor transmission rate (WVTR) was measured using the dry cup method [38]. Aluminum sample cups, equipped with rubber
o-rings, were partially filled with phosphorous pentoxide, a thin film of the polymer sample was placed over the sample cups and a top secured above. The mass of the cup with the pentoxide and the polymer film was taken, and the sample placed into a sealed chamber which was maintained at 90% relative humidity and 23 °C. The weight of the samples was taken every 24 h, over a minimum of 7 days.

### 2.8. Transmission electron microscopy (TEM)

The size of the nanoparticles and their dispersion into the polymer was determined by transmission electron microscopy using a Phillips Model CM100 operated at 80 kV TEM, and high resolution transmission electron microscopy (HRTEM) on a FEI-Tecnai G2 F20 S-Twin HRTEM microscope equipped with a Field Emission Gun (FEG) operating at an accelerator voltage of 120 kV. Samples of the silica nanospheres were prepared for TEM analysis by suspending 0.05 g of nanospheres in 15 mL ethanol and sonicating at 50 °C for 60 min. A drop of the resulting suspension was then placed on a copper TEM grid and allowed to dry.

Samples of the polymer composites were prepared for TEM analysis by melt pressing the materials into molds with dimensions of approximately 10 × 8 × 3 mm, at 190 °C. The nanocomposite samples were then cut to 70 nm of thickness using a Reichert–Jung (Leica) Ultracut ultra microtome with a diamond knife and put onto a 300 mesh copper grid.

## 3. Results and discussion

### 3.1. Nanosphere synthesis and characterization

The principle goal of this research was the production of polypropylene nanocomposites containing silica nanospheres of different diameters. Therefore, the first step was the synthesis of monodisperse silica nanoparticles over a range of sizes. The initial synthesis work focused on batch methods which had previously been developed and reported by our laboratory [12]. The method was found to produce spheres with very small diameters (12 nm), Fig. 1A, but required very long reaction times (20 h). In addition this reaction, for uncertain reasons, was found to be susceptible to gelling which resulted in the formation of solid silica sols, making variations to the procedure difficult. The use of a modified semi-batch method, allowed for the production of larger particles, up to 70 nm, Fig. 1B, and the time of the reaction could be decreased to 2 h. The product diameters of this reaction were found to be more dispersed, however, typically formed bi- and tri-modal distributions. It was suspected that the multimodal distribution was likely due to the semi-batch nature of the reaction as it was not observed in the batch reaction. Therefore, the original batch procedure was modified, by shortening the reaction time (to 2 h) and ODA and water concentrations were varied, permitting the size of the nanoparticles to be varied over a greater range and without the sensitivity to gelling observed in the initial procedure. The use of the surfactant, ODA in this instance, which is often a nuisance it must be removed by calcination, was actually necessary in order to compatibilize the mixture of the polypropylene with the nanospheres. It has been reported that when nanospheres, sans surfactant, were mixed with polypropylene, the spheres did not disperse well due to the strong interaction between the nanospheres and the poor interaction with the hydrophobic polymer matrix [12,39].

The materials used and the size of the particles obtained are shown in Table 1, and the TEM images of the nanoparticles in Fig. 2A–E. As can be observed, a range of sizes can be obtained solely by varying the concentration of the surfactant. The use of a low concentration of surfactant, 0.297 mmol ODA, generates 12 nm nanospheres, increasing the concentration results in larger spheres of up to 150 nm, although the relationship between ODA concentration and sphere size is not well correlated. It was found that the mid-range concentrations of ODA produced the most dispersed nanospheres; compare Fig. 2A with Fig. 2B–D. Smaller spheres appeared to agglomerate more, with the smallest spheres (12 nm) being difficult to find isolated or even in small clusters. It addition, upon observation via HRTEM, Fig. 3, the smaller spheres did not have a well defined spherical shape like the large nanoparticles. One particularly surprising result is the that spheres which measure 150 nm in diameter, upon closer inspection actually are formed from smaller, ca 10 nm, spheres which themselves have assembled into the larger agglomerate sphere, Fig. 2E. This was not an isolated occurrence, and was associated with synthesis in which the ODA concentration was high compared to TEOS. Larger, ca. 200 nm spheres, have also been found to form from smaller ca 35 nm spheres (Fig. 3D).

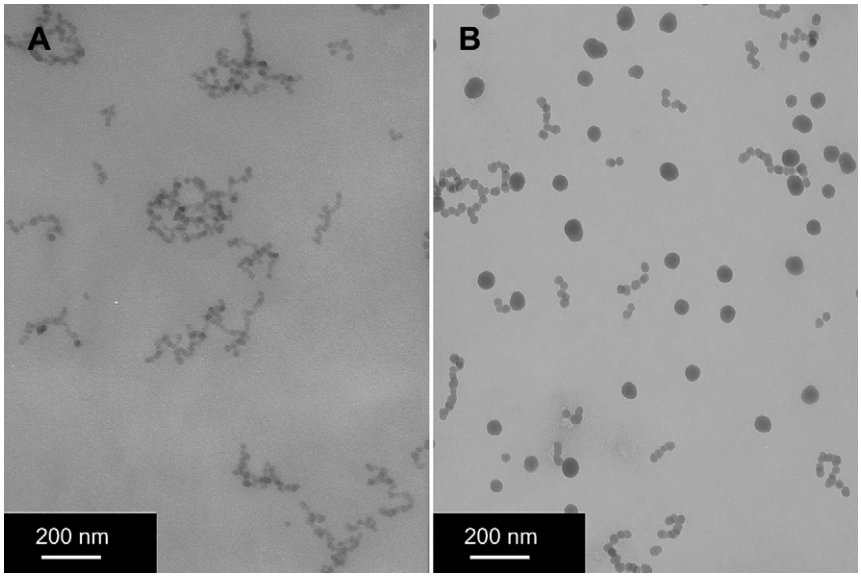


**Fig. 1.** TEM images of nanospheres synthesized by A) batch method and B) semi-batch method.

### 3.2. Thermal properties of the composites

In many instances, the changes to physical properties to a polymer matrix upon addition of inorganic fillers can be explained by differences in the thermal properties of the resulting mixture. Changes in the crystallinity, melting and crystallization temperature and enthalpies of crystallization can result in large differences in the final properties of the polymer. It was suspected that the nanospheres could be acting as nucleating agents and as result, greatly influence the properties of the composites. Therefore, the thermal properties of the composite materials were analyzed and the results summarized, Table 2. The melting

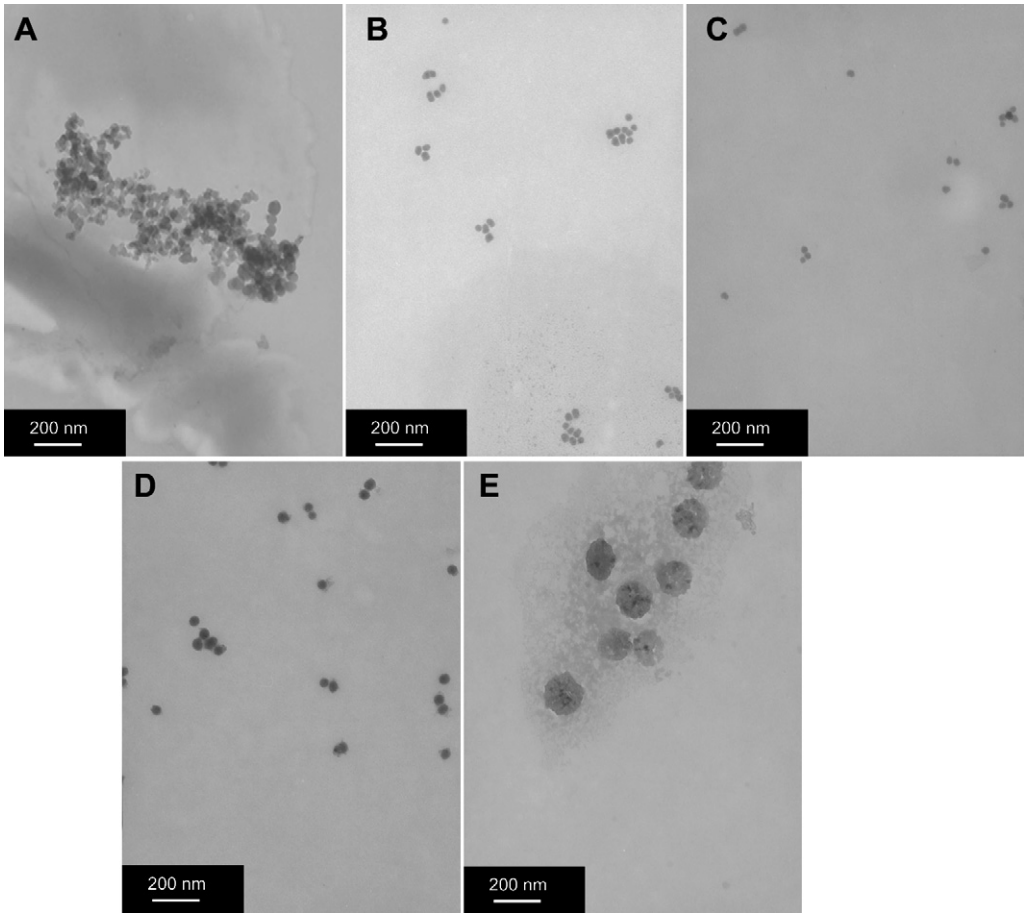


**Fig. 2.** TEM images of nanospheres in solution. A) 12 nm; B) 30 nm; C) 36 nm; D) 44 nm; E) 150 nm.

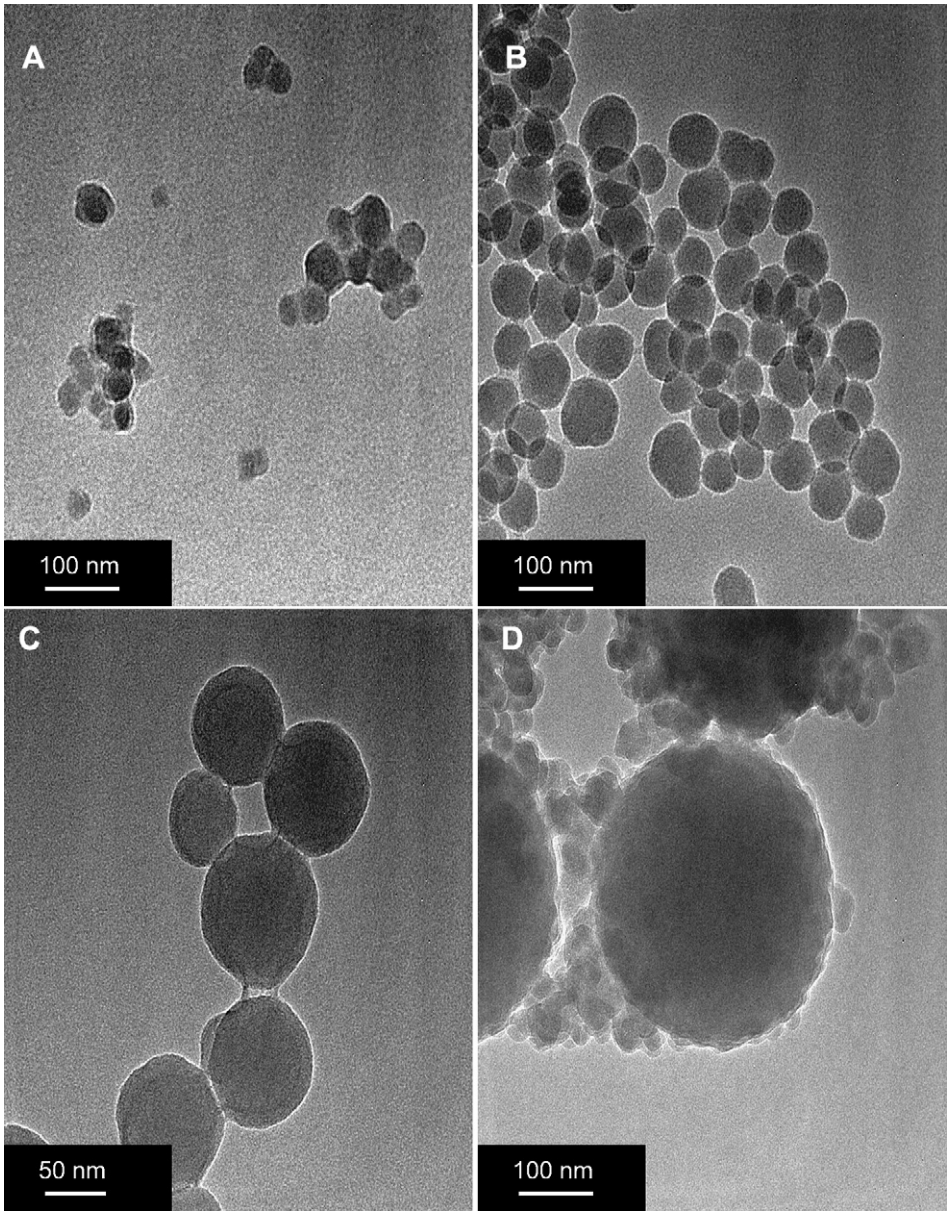


**Fig. 3.** High resolution TEM Images of selected nanospheres in solution: A) 30 nm; B) 44 nm; C) 70 nm; D) 200 nm.

temperature of all the nanocomposites decreased in comparison to the pure polymer as well as the mixture of polypropylene and polybond. This decrease varied in the samples from 1 to 3 °C without any particular trend. The onset crystallization temperature of the composites produced with PP26 decreased by 2–3 °C, DSC traces shown in Fig. 4, while that of the composites produced with PP13, Fig. 5, did not change (a 1 °C change in one instance). The different behaviors in the onset crystallization of the two types of polypropylenes indicate that the higher melt flow index polypropylene (PP26) is more intimately incorporating the nanospheres, as indicated by their greater effect. The decrease in crystallization indicates that the nanospheres are not acting as nucleating agents and that they in fact may be hindering the crystallization process, either through their presence alone or through that of the surfactant associated with them, in any case the effect is minimal.

**Table 2**
Thermal properties of the polypropylene nanocomposites.

| Sphere diameter (nm) | PP26 | | | PP13 | | |
|---|---|---|---|---|---|---|
| | $T_c$ (°C) | $T_m$ (°C) | $X_c$ (%) | $T_c$ (°C) | $T_m$ (°C) | $X_c$ (%) |
| – | 126 | 163 | 64 | 123 | 163 | 61 |
| 12 | 125 | 160 | 64 | 122 | 159 | 64 |
| 30 | 123 | 162 | 68 | 123 | 163 | 58 |
| 36 | 123 | 160 | 64 | 123 | 161 | 62 |
| 44 | 123 | 161 | 66 | 123 | 162 | 64 |
| 70 | 124 | 162 | 65 | 123 | 161 | 65 |
| 150 | 124 | 162 | 67 | 123 | 161 | 64 |

$T_c$: Onset crystallization temperature; $T_m$: Melting temperature; $X_c$: Percent crystallinity.

### 3.3. Mechanical properties

It was suspected that the differences in the viscosities of the two polypropylenes would affect the dispersion of the silica nanoparticles into the polymeric matrix, the higher melt flow index polymer (PP26) being less viscous under the processing conditions,

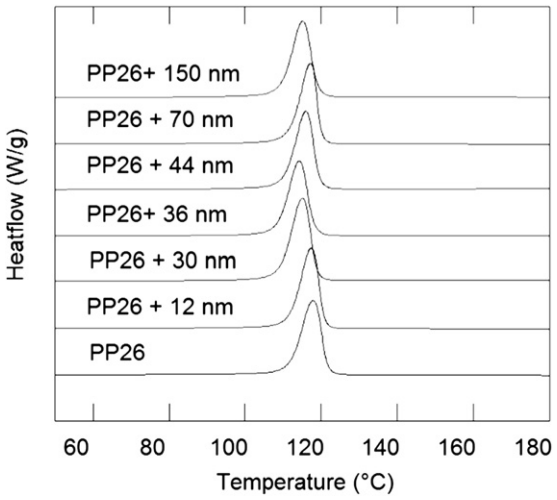


**Fig. 4.** DSC traces of PP26 nanocomposites (exotherm up).

and as such should result in higher quality composites. The results for the mechanical property analysis are shown in Table 3. An average increase in the Young's modulus in the PP26 nanocomposites of about 15% was observed. There is variation in this increase depending on the nanoparticles used, however no clear trend is observed, with the composites produced with the 30 nm spheres showing an increase in Young's modulus of 21%, while those with 44 nm spheres an increase of 16%, and finally the smallest spheres, 12 nm an 11% increase. The elongation at break, which often decreases in polymer composites showed small decreases in almost all samples, with only 1 sample maintaining the original value.

The incorporation of the spheres into PP13 polymer matrix resulted in increases of less than 10% in the Young's modulus, which was lower than that observed in the samples produced with PP26. The strain at break of the composites was perhaps the most telling, with the smallest spheres producing a net decrease in the strain at break of nearly 50%. Samples with larger spheres (44, 36 and 30 nm) had strain at breaks which were ca. 30, 18, and 18% lower respectively. Surprisingly, the sample containing the 150 nm agglomerated spheres had a net increase in the strain at break of ca. 8%. This is surprising as the incorporation of inorganic materials

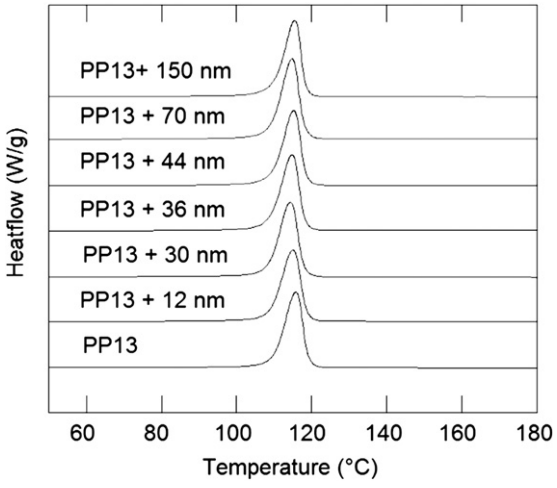


**Fig. 5.** DSC traces of PP13 nanocomposites (exotherm up).

**Table 3**
Mechanical properties of the polypropylene nanocomposites.

| Sphere diameter (nm) | PP26 | | PP13 | |
|---|---|---|---|---|
| | Young's modulus (MPa) | Elongation at break (%) | Young's modulus (MPa) | Elongation at break (%) |
| – | 1123 | 7 | 1076 | 8 |
| 12 | 1252 | 4 | 1063 | 4 |
| 30 | 1361 | 7 | 1107 | 7 |
| 36 | 1305 | 4 | 1148 | 7 |
| 44 | 1316 | 5 | 1147 | 6 |
| 70 | 1170 | 7 | 1098 | 7 |
| 150 | 1326 | 5 | 1085 | 9 |

Error: 10%; Spheres content: 1 wt%.

into polyolefins typically results in a decrease in their strain at break even at very low loadings.

In summary, the silica nanospheres appear to have little effect on the mechanical properties, which was expected as their aspect ratio is very low (ca. 1).

### 3.4. $O_2$ and $N_2$ permeability of the composites

The permeability results of the polymers and polymer composites are shown in Table 4. The permeability of the composites to both $O_2$ and $N_2$ increased in almost all of the nanocomposites samples, and the permeability increased with respect to the nanoparticle diameter. The two gases however had different trends, with the $O_2$ permeability increasing at twice rate of the $N_2$ permeability, 26 and 13 percent for PP26, and 25 and 12 percent for PP13, for the samples with the largest nanosphere diameter. It has previously been reported that the addition of very small spheres, ca 1–10 nm, results in a reduced permeability due to a tortuous path mechanism [31,40]. Indeed, a reduction in the permeability of the composites containing the smaller spheres was observed (12 nm). However, the samples containing the larger nanospheres had increased permeability. The difference is due to the quality of the dispersion of the materials, the 12 nm spheres (Fig. 6A) formed larger aggregates. If the spheres are not well dispersed, then they no longer behave as small, solitary particles, but rather as larger barriers to permeability via tortuous path type mechanisms. The larger spheres were found to be better dispersed, Fig. 6B, and while they may add to the path tortuosity, it appears that there are secondary contributions which outweigh that effect. It has been observed that the addition of nanospheres results in the formation of voids, generating free volume through which the penentrants can travel freely. This explains the increase in oxygen permeability as the kinetic diameter of oxygen is smaller (3.46 Å), and as such an increases to the diffusivity would impact is permeability more so than the larger nitrogen (3.64 Å) [40].

**Table 4**
Permeability of the polypropylene nanocomposites.

| Sphere diameter (nm) | PP26 | | | PP13 | | |
|---|---|---|---|---|---|---|
| | $PO_2$ (Barrer) | $PN_2$ (Barrer) | Selectivity $O_2/N_2$ | $PO_2$ (Barrer) | $PN_2$ (Barrer) | Selectivity $O_2/N_2$ |
| – | 1.13 | 0.58 | 2.0 | 1.95 | 0.67 | 2.9 |
| 12 | 0.99 | 0.55 | 1.8 | 1.92 | 0.65 | 3.0 |
| 30 | 1.21 | 0.62 | 2.0 | 2.11 | 0.69 | 3.0 |
| 36 | 1.29 | 0.62 | 2.0 | 2.25 | 0.75 | 3.0 |
| 44 | 1.31 | 0.63 | 2.1 | 2.35 | 0.77 | 3.0 |
| 70 | 1.37 | 0.64 | 2.1 | 2.53 | 0.75 | 3.4 |
| 150 | 1.42 | 0.65 | 2.2 | 2.55 | 0.76 | 3.4 |

P: Permeability coefficient; Sphere content: 1 wt%; Pressure: 2 bar.

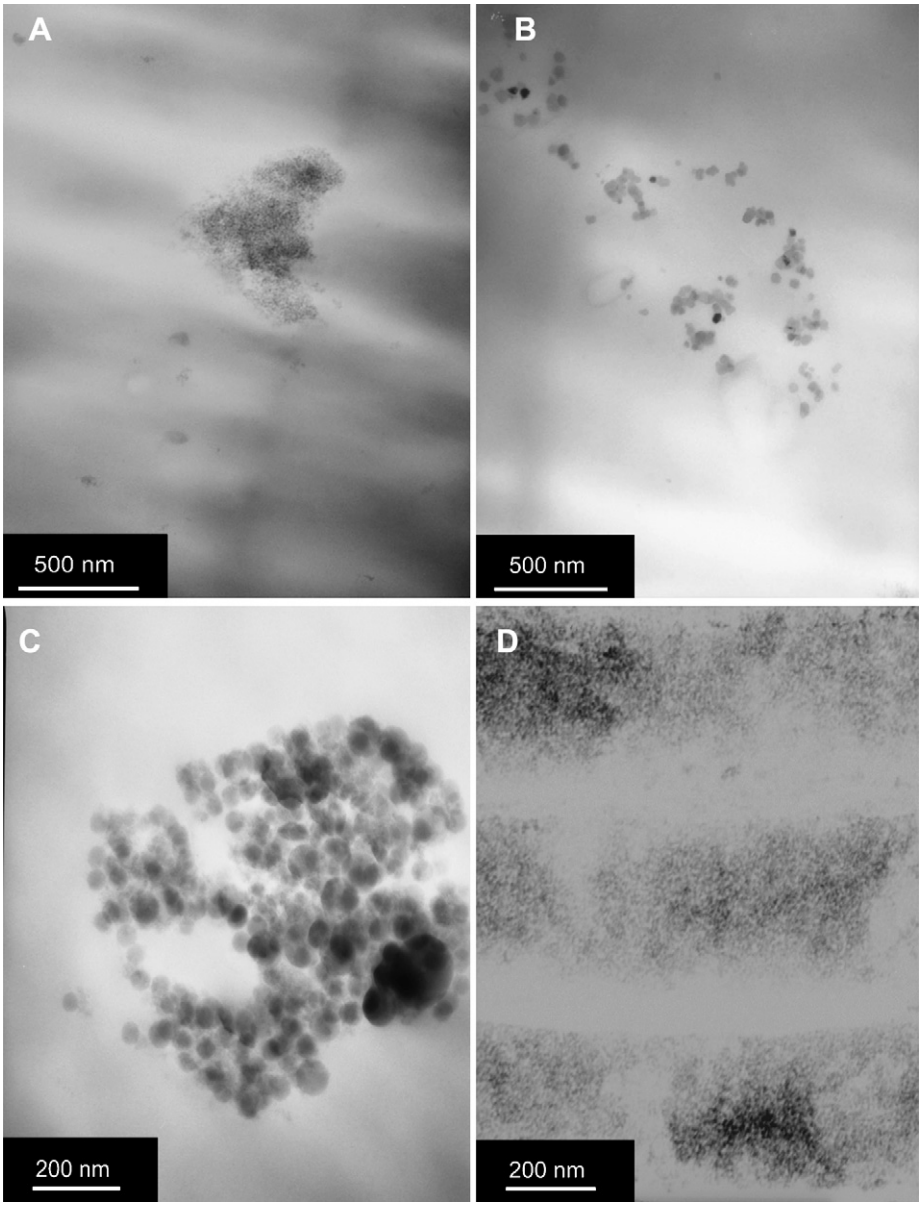


**Fig. 6.** TEM Images of selected polypropylene nanocomposites: A) PP26 + 12 nm; B) PP26 + 70 nm; C) PP13 + 70 nm and D) PP13 + 12 nm.

In theory, the compatibilizer should reduce the formation of voids by improving the compatibility between nanospheres and polymer. This is indeed the case, when composites were produced without the use of compatibilizer, using the 44 and 70 nm nanospheres and PP26, it was found that the oxygen and nitrogen permeability increased substantially. The permeability of the 44 nm/PP26 composites increased 49 and 80% for oxygen and nitrogen (1.95 and 1.12 barrer) respectively, while the 70 nm/PP26 composites increased 71% and 103% for oxygen and nitrogen (2.35 and 1.31 barrer) respectively. It is clear that due to the incompatible natures of the polypropylene and silica, a compatibilizer is required to disperse the nanoparticles into the PP matrix. The permeability of the composites produced without Polybond, however, demonstrate that the use of a compatibilizer is required in order to achieve a good compatibility and reduce the formation of voids.

One potential factor which can greatly affect the permeability of the samples is their crystallinity. The $X_c$ of the composites all show a slight increase, Table 2, this change, however, should decrease the permeability, whereas an increase is observed, therefore the effect of the crystallinity on the permeation behavior of the composites is suspected to be minimal.

### 3.5. Water vapor transmission rate (WVTR)

The incorporation of nanospheres into the polypropylene matrix resulted in an increased water vapor transmission rate in both polypropylene matrices, Figs. 7 and 8 show the trends observed. This increase was found to be inversely proportional to the nanosphere diameter and scaled roughly with the surface area per unit volume ($3/r$) of the spheres, which suggests that the water vapor is adsorbing on the silica nanosphere surface, thereby increasing its solubility in the matrix. This behavior has previously been observed in polypropylene–clay composites prepared using PP-g-MA as a compatibilizer [41]. This increase was attributed to the clay surface affinity for water, which can adsorb water resulting in an increase in the solubility of water in the polymer composite. The formation of channels between adjacent particles in systems with poor dispersion further increases the water vapor transmission

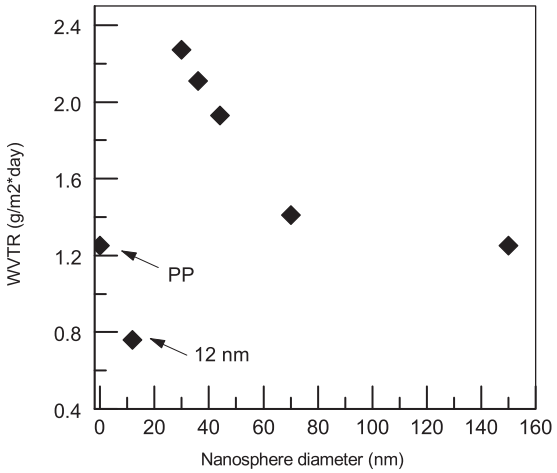


**Fig. 7.** Water vapor transmission rate of the PP26 nanocomposites, PP in this graph is a mixture of PP26 with Polybond in the same ratio as used in the composites.

rate. The increase in water vapor transmission rate upon the addition of smaller (30 nm) spheres to the polypropylene matrices resulted in a substantial increase in the water vapor transmission of 80–90 percent compared to the two polypropylene matrices. The water vapor transmission rate of the polypropylene matrices decreases when the diameter of the nanospheres is increased. Increasing the diameter of the spheres by 20, 45, and 133 percent, to 36, 44 and 70 nm respectively, resulted in a net increase in the water vapor transmission rate compared to the polypropylene/polybond blend, however, the composites showed reduced transmission compared to the smaller nanospheres. Again, it is observed that the composites with the 12 nm spheres show a different behavior in comparison with the other particles, likely due to their high agglomeration which causes them to have a low surface area to volume ratio. The two polypropylenes behave similarly in the tests, however the higher molecular weight material, PP13 has a lower initial transmission rate by 0.25 g/m$^2$ day, and this difference is more or less maintained throughout the samples.

### 3.6. Effect of weight loading

The effect of nanosphere content in one of the polypropylene matrices (PP26) was also studied using silica nanosphere weight loadings of 3 and 5 wt%. Samples were prepared using PP26 and 30 nm spheres. The 30 nm spheres were chosen due to their permeability behavior, they were the smallest spheres to produce an increase in permeability, with the expectation that the increase in the permeability would be maintained or augmented at higher loadings. The thermal properties indicate that the incorporation of additional nanospheres does not affect the melting and crystallization temperature compared to the 1 wt% samples. The values obtained for the nanocomposites obtaining 3 wt% and 5 wt% were $T_c$: 126 °C and 128 °C, and $T_m$: 162 °C and 163 °C, respectively, the DSC traces are shown in Fig. 9. The percent crystallinity shows little change 68% (3 wt%) and 63% (5 wt%). The modulus of the polymer composites do not change significantly with the increase in loading, with the 3 wt% composite having a Young's modulus of 1013 MPa and the 5 wt% a Young's modulus of 1065 MPa. This represents a decrease compared to the 1 wt% composite but is equal to that obtained for the pure PP26.

The oxygen permeability of the composites containing 3 and 5 wt% nanospheres was found to increase from 1.21 barrer for the 1 wt% composites, to 1.50 and 1.71 barrer for the 3 and 5 wt% composites, respectively. The nitrogen permeability increased in the sample by 50% with the nitrogen permeability of the 5 wt% sample increasing to 0.91 barrer.

The water vapor transmission rate shows an increase when the nanospheres content is increased reaching values of 3.53 g/m$^2$·day for the nanocomposites with 3 wt% and a value of 4.24 g/m$^2$·day using 5 wt% of nanospheres. This represents an increase of 56% and 86% respectively compared to composite with 1 wt% nanospheres. This increase is likely due to an increase in the silica surface area in the composites, which increases the solubility of the water vapor, as well as an increased propensity to form channels between the particles as the weight loading increases.

### 3.7. Effect of polymer molecular weight on resulting composite materials

It was thought that the selection of two polypropylenes with differing molecular weights would result in different behaviors when composited with the nanoparticles. The physical properties of the composite materials support this conclusion; the Young's modulus of the PP26 composites increased an average of 165 MPa (15%) while the composites of the PP13 composites increased an average of 32 MPa (3%). The absolute increase in permeability of the PP13 composites ($PO_2$ average increase of 0.41 barrer) was twice

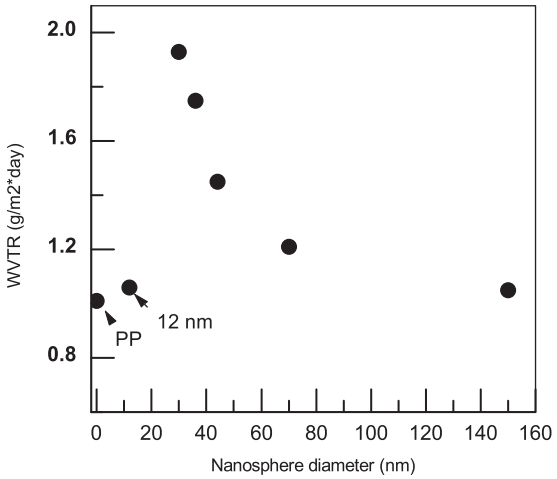


**Fig. 8.** Water vapor transmission rate of the PP13 nanocomposites PP in this graph is a mixture of PP13 with Polybond in the same ratio as used in the composites.

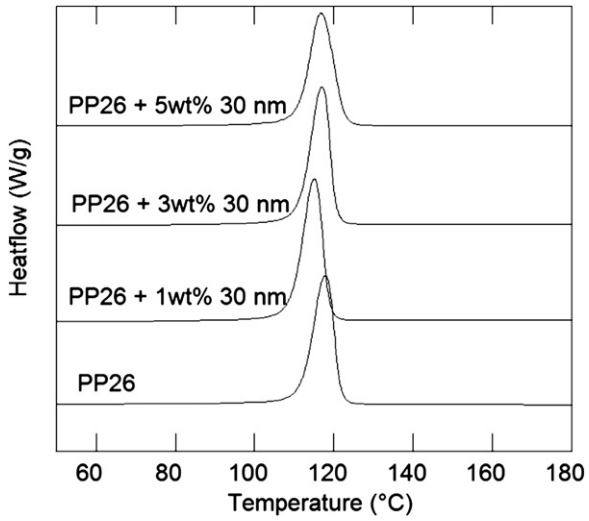


**Fig. 9.** DSC traces of PP26 nanocomposites with different weight loadings of silica nanospheres (exotherm up).

that observed for the PP26 composites ($PO_2$ average increase of 0.19 barrer), this larger increases is likely due to greater void formation, associated with poorer compatibility between the particles and the polymer matrix. The difference in the quality of dispersion can be observed in Fig. 6A–D. The composites prepared with PP13 showed poorer dispersion and larger aggregates compared to PP26 under the processing conditions used.

## 4. Conclusion

In this contribution we have reported on the synthesis of monomodal silica nanospheres and their incorporation into polypropylene nanocomposites using two polypropylenes of different molecular weights. These materials were found to possess increased modulus and decreased strain at break compared to the virgin material. The addition of the nanoparticles did not significantly alter the thermal properties of the polypropylene matrix. The $O_2$ and $N_2$ permeability of the composites was found to increase (when the spheres were well dispersed) in correlation with the nanosphere diameter. It was found that the selectivity of the polymers towards oxygen increased, likely due to increased diffusivity. The water vapor transmission rate was found to show the greatest dependence on the radii of the spheres, with the smaller spheres nearly doubling the initial transmission rate. These results illustrate that the diameter of nanospheres can play a critical role in the final properties of the materials and that to a limited extent the permeability and physical properties of the materials can be controlled by controlling the size of the nanospheres added. The addition of higher weight loadings, to 3 and 5 wt%, of nanospheres resulted in increased water and gas permeability without a reduction in physical properties. The PP with the higher MFI proved to produce higher quality dispersions, indicating that matrix selection is important in producing quality nanocomposites.

## Acknowledgement

The authors wish to thank to CONICYT for the financing of this work, through project FONDAP 11980002 and for the Ph.D. and AT24090014 scholarships of V. Dougnac. They also wish to acknowledge the assistance of Dr. D. Serafini (USACH) and P. Quevedo with the DSC analysis and Dr. W. Sierralta (INTA) for the TEM images.

## References

[1] Paul DR, Robeson LM. Polymer 2008;49(15):3187–204.
[2] Francesco C, Serena C, Elisa P, Andrea P, Giacomo R. Nanocomposites Based on Polyolefins and Functional Thermoplastic Materials 2008;57:805–36.
[3] Brown GE, Blackwell JW. Composition of Matter for Soles of Shoes. USPTO, 460,842, USA; 1891.
[4] Alexandre M, Dubois P. Materials Science and Engineering: R: Reports 2000;28 (1–2):1–63.
[5] Maier C, Calafut T. Polypropylene: the definitive user's guide and databook. William Andreu Publishing/Plastics Design Library; 1998. p. 49.
[6] Tjong SC, Li RKY. Journal of Vinyl and Additive Technology 1997;3(1):89–95.
[7] Toro P, Quijada R, Arias JL, Yazdani-Pedram M. Macromolecular Materials and Engineering 2007;292(9):1027–34.
[8] Dimitris NB, George ZP, Eleni P, Nikolaos V, Paraskevas P, George PK. 2006;100 (4):2684–2696.
[9] Maurizio A, Simona C, Maria Laura Di L, Emilia Di P, Maria Emanuela E, Gennaro G. Macromolecular Symposia 2006;234(1):156–62.
[10] Moncada E, Quijada R, Lieberwirth I, Yazdani-Pedram M. Macromolecular Chemistry and Physics 2006;207(15):1376–86.
[11] Yun SK, Maier J. Inorganic Chemistry 1999;38(3):545–9.
[12] Moncada E, Quijada R, Retuert J. Nanotechnology 2007;18:0957–4484.
[13] Nakamura H, Matsui Y. Journal of the American Chemical Society 1995;117 (9):2651–2.
[14] Yu K, Guo Y, Ding X, Zhao J, Wang Z. Materials Letters 2005;59 (29–30):4013–5.
[15] Hench LL, West JK. Chemical Reviews 2002;90(1):33–72.
[16] Kim KD, Kim HT. Journal of Sol-Gel Science and Technology 2002;25 (3):183–9.
[17] Chen Y, Zhou S, Chen G, Wu L. Progress in Organic Coatings 2005;54(2):120–6.
[18] Stöber W, Fink A, Bohn E. Journal of Colloid and Interface Science 1968;26 (1):62–9.
[19] Maged AO, Vikas M, Ulrich WS. Macromolecular Chemistry and Physics 2007;208(1):68–75.
[20] Frounchi M, Dadbin S, Salehpour Z, Noferesti M. Journal of Membrane Science 2006;282(1–2):142–8.
[21] Mirzadeh A, Kokabi M. European Polymer Journal 2007;43(9):3757–65.
[22] Mittal V. European Polymer Journal 2007;43(9):3727–36.
[23] Villaluenga JPG, Khayet M, López-Manchado MA, Valentin JL, Seoane B, Mengual JI. European Polymer Journal 2007;43(4):1132–43.
[24] Naoki H, Arimitsu U. Journal of Applied Polymer Science 2004;93(1):464–70.
[25] Gorrasi G, Tortora M, Vittoria V, Kaempfer D, Mülhaupt R. Polymer 2003;44 (13):3679–85.
[26] Lew CY, Murphy WR, McNally GM. Polymer Engineering and Science 2004;44 (6):1027–35.
[27] Zou H, Wu S, Shen J. Chemical Reviews 2008;108(9):3893–957.
[28] Merkel TC, Freeman BD, Spontak RJ, He Z, Pinnau I, Meakin P, et al. Science 2002;296(5567):519–22.
[29] Takahashi S, Paul DR. Polymer 2006;47(21):7519–34.
[30] Takahashi S, Paul DR. Polymer 2006;47(21):7535–47.
[31] Alexandros V, Dimitrios B, Eleni P. Macromolecular Reaction Engineering 2007;1(4):488–501.
[32] Sen TZ, Sharaf MA, Mark JE, Kloczkowski A. Polymer 2005;46(18):7301–8.
[33] Xue L, Borodin O, Smith GD. Journal of Membrane Science 2006;286 (1–2):293–300.
[34] Zhou J-H, Zhu R-X, Zhou J-M, Chen M-B. Polymer 2006;47(14):5206–12.
[35] Canevarolo S, Candia FD. Journal of Applied Polymer Science 1995;57 (5):533–8.
[36] Koros WJ, Paul DR, Rocha AA. Journal of Polymer Science: Polymer Physics Edition 1976;14(4):687–702.
[37] O'Brien KC, Koros WJ, Barbari TA, Sanders ES. Journal of Membrane Science 1986;29(3):229–38.
[38] Saito R, Hosoya T. Polymer 2008;49(21):4546–51.
[39] Kazuo A, Boping L, Minoru T, Koh-hei N. Macromolecular Rapid Communications 2006;27(12):910–3.
[40] Vladimirov V, Betchev C, Vassiliou A, Papageorgiou G, Bikiaris D. Composites Science and Technology 2006;66(15):2935–44.
[41] Dumont MJ, Reyna-Valencia A, Emond JP, Bousmina M. Journal of Applied Polymer Science 2007;103(1):618–25.